An Investigation of the Causes that Lead to Burn-In/Burn-On in Heavy Section Steel Castings

B.L. Kruse, V.L. Richards, P.D. Jackson
University of Missouri-Rolla, Rolla, Missouri

ABSTRACT

The causes of burn-in/burn-on have been the subject of research for many years (Asanti 1966 and Chernogorov 1970). It has been attributed to vapor penetration, liquid iron silicate formation and mechanical penetration mechanisms. These mechanisms were considered and a series of designed experiments were performed using no-bake molds with the following variables: compaction technique, sand reclamation method, coating process and work time. The quantitative results of these experiments were explained by further investigation using microstructural and chemical analysis. The overall goal of these experiments was to try to understand the suspected causes of burn-in/burn-on associated with heavy section steel castings. The condition of the sand supporting the coating was found to be critical.

INTRODUCTION

Surface defects caused by metal-mold interactions have been the subject for debate for many years. Traditionally, surface casting defects in steel and iron castings typically have been classified as either burn-in or burn-on depending upon the whether or not there was a recognizable glassy phase (burn-in) in the defect. However, the foundries that were involved in this study employed a different classification system that ranked surface defects by ease of removal, similar to the definitions of burn-in, burn-on and mechanical penetration listed in the *International Atlas of Casting Defects* (Rowley 1993). These sources designated burn-on as the most severe adhering sand defect because it required grinding for removal while burn-in was any adhering sand defect that could be chipped off and was less severe than the thicker metal penetration. In all three cases, these surface defects were normally found in the hottest locations of the casting (Rowley 1993) and could not be removed by normal non-labor intensive methods such as shot blasting.

In steel castings, Svoboda (1994) related these surface defects to three categories and gave a quantitative assessment on the relative frequency of occurrence as:

1) Liquid-state penetration – 75%
2) Chemical-reaction penetration – 20%
3) Vapor-state penetration -5%

However, work on the viability of vapor penetration using global free energy minimizing software packages has cast doubt on this as an actual mechanism (Richards and Monroe 1999). Furthermore, because of the low occurrence of 5% listed by Svoboda (1994), vapor-state penetration will not be considered as a factor in the surface defects discussed in this paper.

The work reported here is a synopsis of several case studies in which the mechanisms behind burn-in, burn-on and penetration were studied and addressed.

EXPERIMENTAL PROCEDURE

SMALL V-BLOCK

This work began with a series of initial case studies (Richards and Rasquinha 2002) of burn-in, burn-on and mechanical penetration in production castings. As the literature (Rowley 1993 and Svoboda 1996) reported, the surface defects were concentrated in areas under or near a riser or at an internal corner because of proximity to the hottest portion of the casting – often called hot spots. Because of this, a test v-block, designated as the "small v-block" in Figure 1, was designed with the help of the participating foundries to simulate the thermal conditions located at these hot spots.

Qualitative trials (not large enough for statistical significance) were performed at three foundries using the small v-block and are summarized in Table 1. The trial at Foundry B sought to examine how the type of sand, whether it is silica, chromite and kyasill would reduce the amount of burn-in Kyasill is the trade name to a low thermal expansion zirconium-aluminum-

silicate product with a high thermal conductivity. The second trial at Foundry E examined the influence of iron oxide on the ability to reduce burn-in with silica sand and using zircon sand with no iron oxide. The final trial at foundry F looked at how varying the amount of iron oxide varied the burn-in.

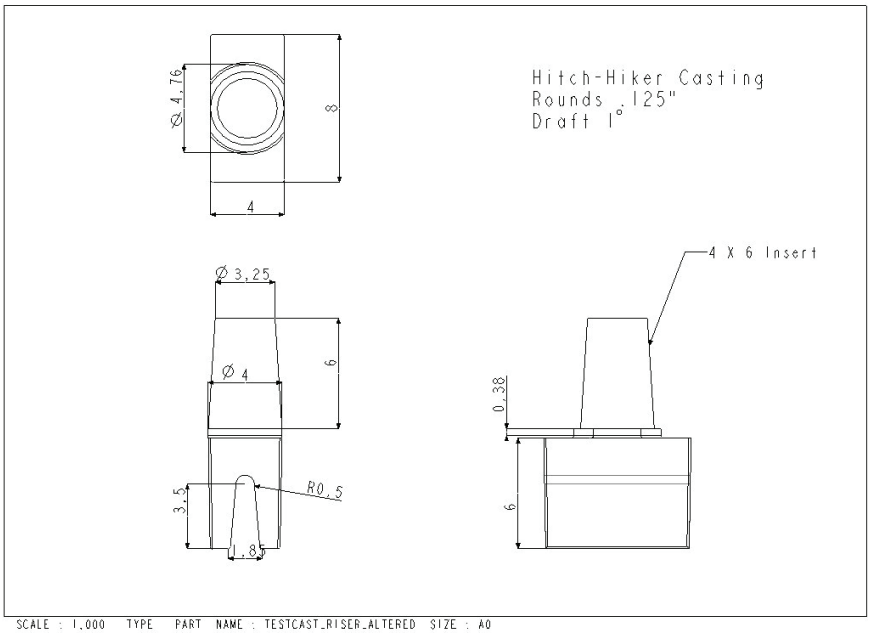

Figure 1: Small v-block casting with direct pour riser

Table 1: Variables for Small V-Block Trials

	Variable	Mold Wash Application	Steel Type
Foundry B	Silica Sand	Spray Coating	Medium Carbon
	Chromite Sand		
	Kyasill		
Foundry E	1% Iron Oxide and Silica Sand	Brush Coating	Low Carbon
	3% Iron Oxide and Silica Sand		
	Zircon Sand (0% Iron Oxide)		
Foundry F	1% Iron Oxide with Silica Sand	Flow Coating	Stainless
	2% Iron Oxide with Silica Sand		
	3% Iron Oxide with Silica Sand		

LARGE V-BLOCK

After the initial experimental results were reported to the Steel Founders' Society of America Carbon and Low Alloy Research Committee, it was suggested that a more aggressive thermal section, such as would be found in even heaver section castings, should be simulated. This then led to the second v-block designated as the large v-block as shown in Figure 2.

The second phase of experiments involved using a two level full factorial on four factors using the new large v-block casting as shown in Table 2. The large v-blocks were poured into furan-bonded molds at one foundry using CF-8C stainless steel.

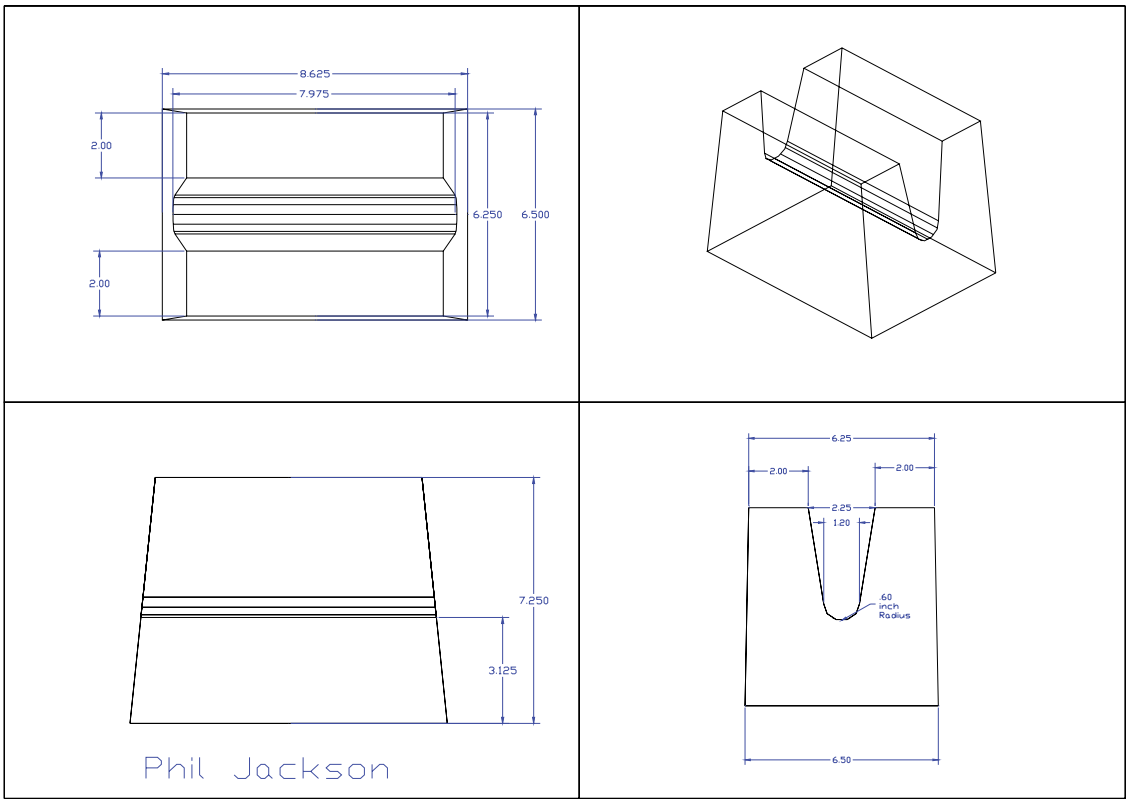

Figure 2: Large v-block casting (shown upside down without the direct pour riser – i.e. drag side up)

Table 2: Variables in the Factorial Experiment Using Large V-Block

Variable	*Level 1*	*Level 2*
Sand	Mechanically and Thermally Reclaimed	Mechanically Reclaimed Only
Compaction	Vibration	Hand Ram
Work time/Strip	Immediate vibration or ramming	Delayed 30 seconds to start after fill
Coating (Zircon Wash)	Flow	Brush

MICROSTRUCTURAL ANALYSIS OF BURN-IN AND PENETRATION IN THE LARGE V-BLOCK DESIGNED EXPERIMENTS

Once the castings were shaken out, the volume and area of burn-in/on and penetration located in each of the notches were measured as shown in Figure 3-A. The castings were then sectioned (Figure 3-B), macro-graphed (Figure 3-C) and mounted in a thermosetting epoxy (Figure 3-D). After polishing the samples with diamond paste, they were examined using an optical microscope and a Hitachi S-570 scanning electron microscope (SEM). Secondary electron images (SE) and back-scattered electron images (BSE) were taken of each of the burn-in areas along with energy dispersive x-ray spectroscopy (EDS) spot analysis and EDS compositional maps in order characterize the burn-in/on and penetration in each of the various factors examined in the second phase of experimentation.

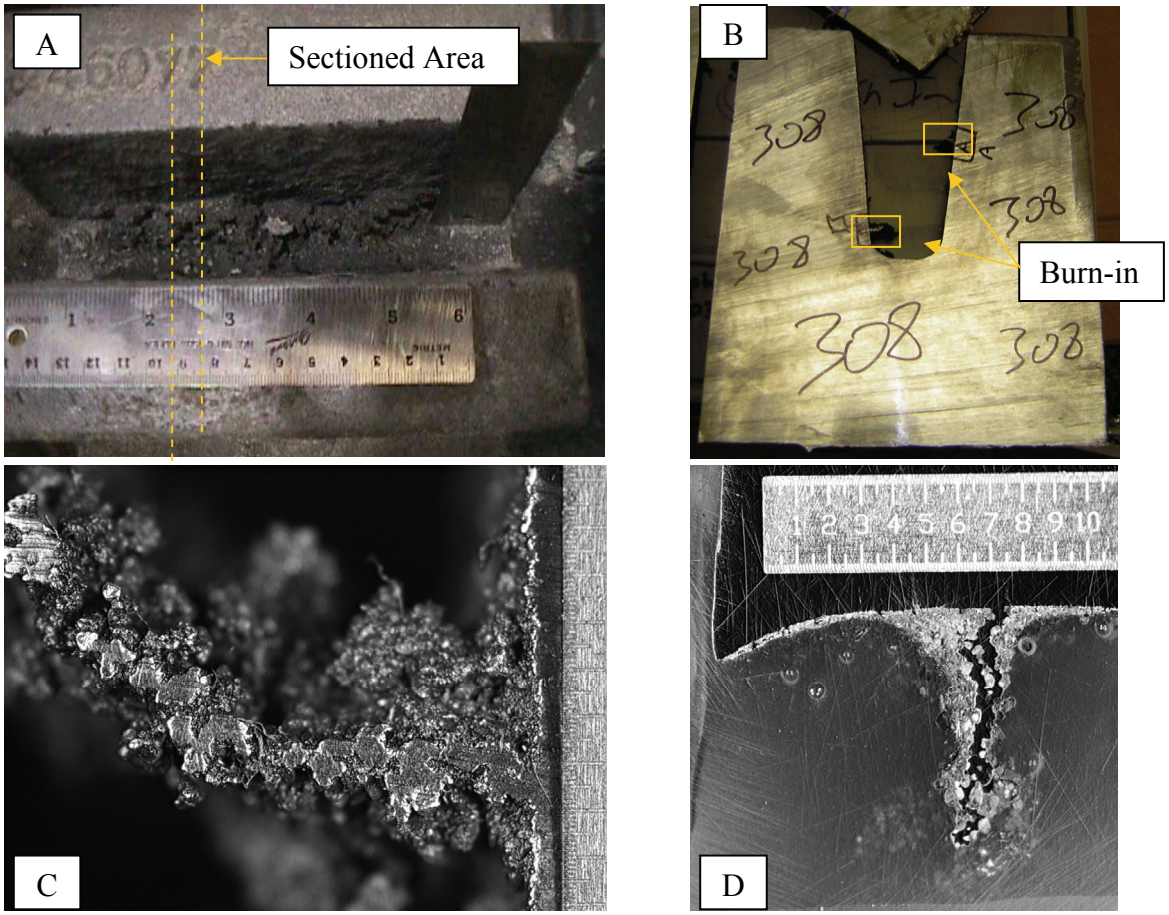

Figure 3: Large v-block casting (A), section of casting (B), macro-image of burn-in (C) and an epoxy mounted burn-in defect (D)

RESULTS AND DISCUSSION

SMALL V-BLOCK

Even though the trials using the small v-block were too small for any statistical significance, the outcomes are of interest and are shown in Table 3. At Foundry B, there were significant amounts of burn-in and veining in the notch when the silica sand was used as a molding material. In addition, burn-in, but not veining appeared in the notch when the chromite sand was used and there were no surface defects in the Kyasill sand. Upon further examining the burn-in in the chromite molded casting, there was evidence of liquid phase sintering. The outcome of the next experiment at Foundry E was that the zircon sand that did not contain any iron oxide and the silica sand with 3% iron oxide could produce a casting without any burn-in or veining while silica sand with 1% iron oxide produced both burn-in and veining. The last set of experiments at Foundry F did not produce any burn-in but there was a reduction in the veining of the casting by using 2% iron oxide.

To better explain why the various molding materials produced a range of burn-in, thermal modeling of the small v-block was performed. Using *Solid Cast*, the temperature 2 mm (0.08 in) from the metal surface of notch was above the solidus of steel for 6.8 minutes when silica sand was used and the pouring temperature was 1593°C (2900°F). When zircon sand was tested under the same conditions, the steel was above its solidus temperature for 2.7 minutes while the chromite sand proved to be so conductive that the steel was never above the solidus temperature. Yet, the results of the chromite molded v-blocks experiment showed liquid phase sintering products in the burn-in area. This may be caused by contaminants in the sand. Depending upon the source, there are varying amounts of iron oxide and silica contents. From these experiments, it can be concluded that the thermal profile is only part of the answer.

Table 3: Outcomeo Small V-Block Experiments

	Variable	Mold Wash Application	Steel Type	Surface Defects
Foundry B	Silica Sand	Spray Coating	Low Carbon	Burn-in and Veining
	Chromite Sand			Burn-in only
	Kyasill			None
Foundry E	1% Iron Oxide and Silica Sand	Brush Coating	Low Carbon	Burn-in and Veining
	3% Iron Oxide and Silica Sand			None
	Zircon Sand (0% Iron Oxide)			None
Foundry F	1% Iron Oxide with Silica Sand	Flow Coating	Stainless	Veining; No Burn-in
	2% Iron Oxide with Silica Sand			Minimum Veining; No Burn-in
	3% Iron Oxide with Silica Sand			Veining; No Burn-in

LARGE V-BLOCK

After the 16 castings were shaken out, the area of burn-in and penetration was visually measured in each of the notches of the large v-blocks as given in Table 4. This seemed to be the most responsive dependent variable to base the analysis of the various conditions. By performing an ANOVA on the process variables, the type of sand proved to be the only significant variable in the cause of burn-in with a 97% significance level as shown in Table 5. The analysis in Figure 4 showed that when the sand was mechanically and thermally reclaiming as opposed only mechanically reclaiming the sand, burn-in was reduced.

Table 4: Listing of Mold Conditions and Burn-In Area (MR/TR = Mechanical Reclaim and Thermal Reclaim, MR = Mechanical Reclaim Only)

Casting Codes	Work/Strip Time	Compaction Method	Sand Type	Coating Application	Burn-in Surface Area (in^2)
22294	immediate	vibration	MR/TR	flow	3.27
22295	immediate	vibration	MR/TR	brush	15.21
22296	delay	vibration	MR/TR	flow	3.10
22297	delay	vibration	MR/TR	brush	4.83
22298	immediate	hand	MR/TR	flow	15.50
22299	immediate	hand	MR/TR	brush	4.57
22300	delay	hand	MR/TR	flow	8.80
22301	delay	hand	MR/TR	brush	4.81
22302	immediate	vibration	MR	flow	15.64
22303	immediate	vibration	MR	brush	16.18
22304	delay	vibration	MR	flow	13.66
22305	delay	vibration	MR	brush	17.00
22306	immediate	hand	MR	flow	19.34
22307	immediate	hand	MR	brush	7.62
22308	delay	hand	MR	flow	6.85
22309	delay	hand	MR	brush	14.35

Table 5: Anova Analysis on the Effect of Variables on the Burn-In Area

Variables	F-Ratio	P-Value
Sand (Mechanical and Thermal Reclaim or Mechanical Reclaim only)	6.21	.030
Compaction Method (Vibration or Hand Ram)	0.12	0.735
Work/Strip Time (Immediate or Delayed)	1.39	.263
Coating Method (Spray or Brush)	0.01	0.939

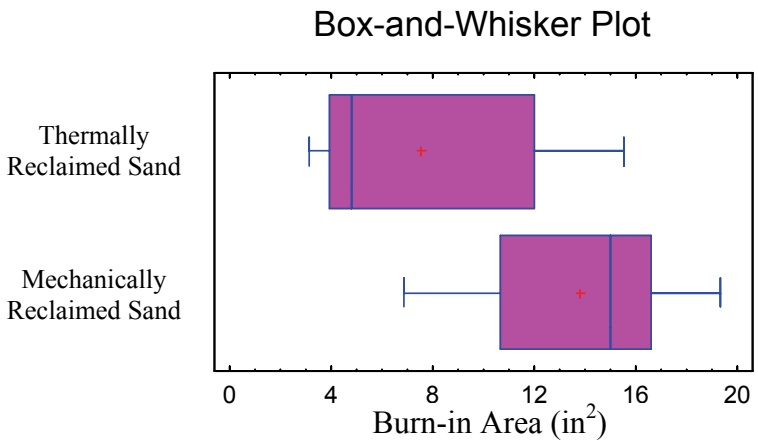

Figure 4: The effect of sand preparation on area of penetration and burn-in on large v-block trial (Thermally reclaimed sand was first mechanically reclaimed)

The effect of thermally reclaiming the sand is further supported by looking at the first study using the small v-block in which the foundries that used all thermally reclaimed sands did not have a problem with burn-in and a clearly defined amount of iron oxide helped to avoid veining.

A study of the compositional and structural effects of mechanical reclamation and thermal reclamation in one of the participating foundries produced some relevant results. The sands were analyzed using energy dispersive x-ray spectroscopy in a scanning electron microscope and the results are demonstrated in Table 6 and Figure 5. Thermally reclaiming the sand allowed for all the remnants of the organic binder, to be burned out as shown in Figure 5B. The burnout is accomplished at a temperature such that the iron and manganese oxides remain unreacted with the silica and can be removed as fines in the cooler/classifier section of the reclamation system. Another advantage is that thermally reclaiming sand allows for an optimum amount of fresh iron oxide to be added to the sand to help with binder breakdown and reduce veining. Mechanically reclaiming does not fully restore sand to its original state and can cause a substantial unknown and uncontrolled buildup of additives and reaction products in the sand.

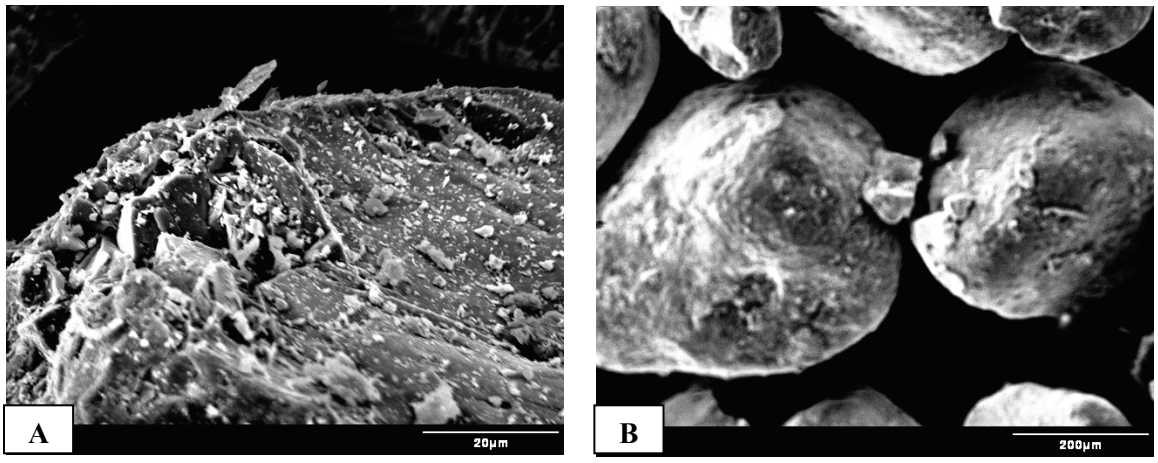

Figure 5: Secondary electron micrograph of a mechanically reclaimed sand grain (A) and a thermally reclaimed sand grain (B)

Table 6: Energy Dispersive X-Ray Spectroscopy Results Demonstrating How Mechanical Reclamation and Then Thermal Reclamation (MR/TR) Differs from Only Mechanical Reclamation (MR) in Spent Foundry Sands

	Al	Si	Mn	Fe	Zr
MR Zircon	0.48	34.09	0.02	2.15	55.17
MR/TR Zircon	0.45	33.92	0.00	0.12	59.75
MR Silica	0.26	18.38	0.00	0.18	0.03
MR/TR Silica	0.32	22.89	0.00	0.02	0.01

MICROSTRUCTURAL ANALYSIS OF BURN-IN AND PENETRATION IN THE LARGE V-BLOCK DESIGNED EXPERIMENTS

The microstructural analysis of the burn-in/on and penetration areas provided a great deal of evidence supporting the thinking that surface defects may be directly related to the condition of the molding media. After looking at many epoxy mounted and polished burn-in and penetration areas, similar features were noticed throughout the defect areas and the areas surrounding the metal intrusion into the mold.

Imaging the metal penetration and burn-in/on was difficult with light optics due to the large contrast between the stainless steel and its entrapped surroundings as shown in Figure 6. The individual sand grains could be seen, but distinguishing between silica, zircon and binder remnants was difficult. Electron microscopy with compositional contrast was a better tool. The SEM allowed for a greater depth of field and contrast, spot chemical analysis and compositional mapping. An example of a secondary electron image of an area of penetration can be seen below in Figure 7 for sample 22305 the utilized vibrated reclaimed sand and a mold wash that was applied with a brush.

Because of the z-contrast associated with secondary electron microscopy and spot analysis, the various structures located in each area of penetration were distinguishable. The zircon coating was not only observed trapped in the burn-in and penetration at the surface, but also in the "fingers" of the metal. This entrapment of zircon is most likely attributed to the rearrangement of the sand once the v-notch portion of the mold was exposed to the heat of the casting.

Figure 6: Micrograph taken from burn-in area of sample 22305

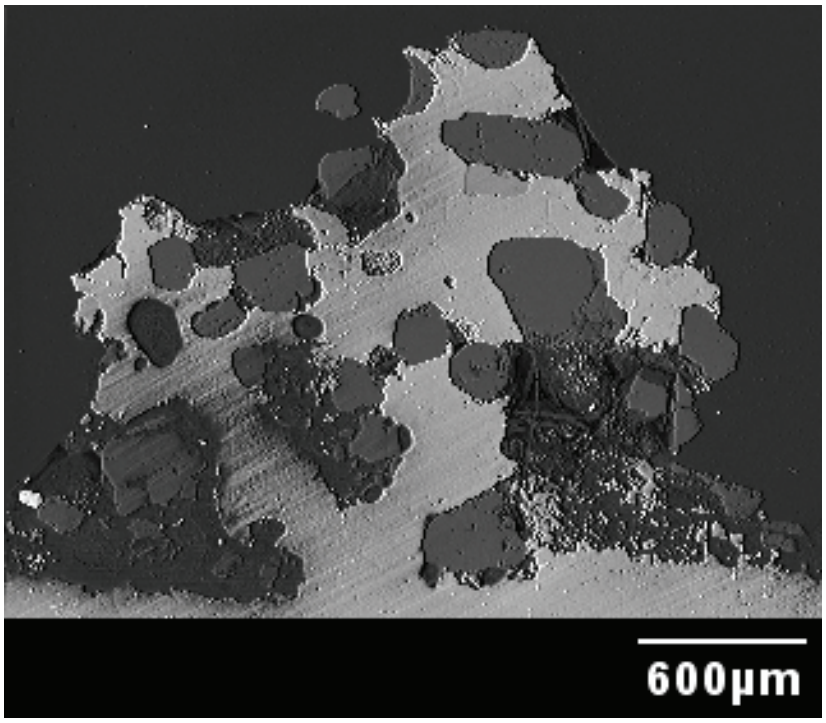

Figure 7: Secondary electron image of burn-in area taken on a Hitachi S-570 SEM at 15kV, working distance of 11mm, and a dwell time of 200ms

Spot chemical analysis and compositional mapping proved to be very productive in the analysis of the penetration and burn-in. From looking at Figure 8, sulfur (yellow) can be seen throughout the area of penetration. Since sulfur is a known wetting agent, this becomes important in looking at the transport mechanism behind penetration. Once the zircon wash coating was breached, the surface tension between the sand grains and the metal was lowered which allowed for an increase in the feeding distance of the penetration. The existence of sulfur in the areas of penetration was especially evident in the samples from the molds that were made with sand that was only mechanically reclaimed and not thermally reclaimed. This is most likely a remnant of the furan binder used in the molding process.

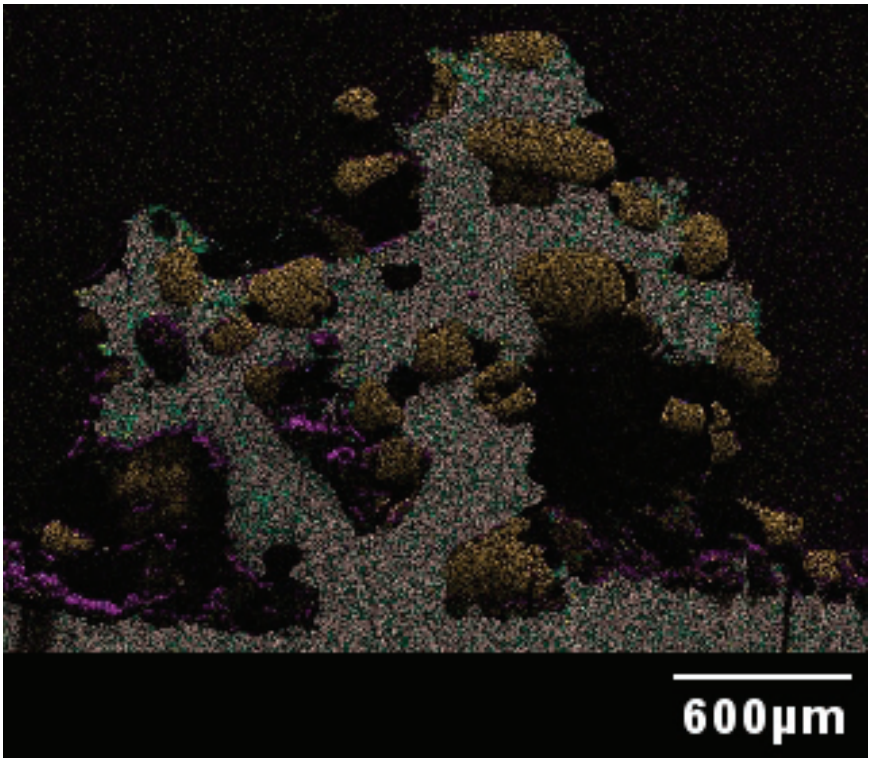

Figure 8: EDS compositional image of entire burn-in area with individual markups of points of interest. Yellow – S, Purple – C, Gray – Fe, Brown – Si, Green - Cr

Upon further examination, a great deal of carbon and other "char" was noted in some of the areas of penetration as shown in purple in Figure 8. This char can be attributed to an excess of non-decomposed binders that would normally be burned out in thermally reclaimed sand. However, when foundries do not fully thermally reclaim their sand, unburned binders, sulfur, iron and other low temperature sintering additives can build-up in the sand system and create serious surface defects in their castings. Therefore, it is no surprise that larger amounts of char, sulfur, iron and manganese were evident in the penetration and burn-in samples taken from molds that were made from sands that were only mechanically reclaimed. The importance of controlling these sand additive remnants and casting by-products is often not fully appreciated. From the previous studies (Richards, 2002), it becomes apparent how just a one percent (of sand weight) fluctuation in the amount of iron oxide can affect the occurrences of penetration and burn-in/on.

MECHANISM OF METAL PENETRATION AND BURN-ON

After looking at the various burn-in/on and penetration samples, a reaction region was observed to be common at the intergranular contact points among the sand grains. An example of this region or intergranular "neck" is shown in Figure 9 and designated as "R" for reaction product. A spot energy dispersive spectrometer (EDS) analysis of the reaction product was performed in order to determine an approximate chemistry as demonstrated in Figure 10. The results of the EDS analysis are also shown below in Table 7. With the chemistry of the reaction product known, the Fact-Sage thermodynamic modeling package was used to investigate the reaction products present at steel pouring temperatures. As shown in Figure 11, at and even below steel pouring temperatures more than 70% of the reaction product is liquid allowing for liquid phase sintering and the rearrangement of the supporting structure of the zircon wash coating.

Liquid phase sintering may partially explain penetration. Zircon washes are effective because they do not allow reactions to occur between the lower melting temperature silica and liquid metal or oxidized surface of the metal. This is schematically illustrated in Figure 12. However, zircon washes are only as effective as their supporting sand. If the sand and its additives below the wash begin to rearrange themselves in order to densify and sinter, the underlying structure may undergo local strain causing mechanical breaks in the zircon wash (Figure 13). The breaks would allow metal penetration or burn-in/on. By controlling the composition of the molding sands, volume reduction and sintering can be minimized; thus, providing a sound substructure to support the zircon wash coating. However, when the sand is only mechanically reclaimed, only the excess fines that contain sand, spent binder, iron oxide and other undesirable oxides can be removed by the air classifier. The remaining sand grains may be coated with unburned binder containing oxide fines as depicted in Figure 13 and shown in Figure 5A. In order to remove all of the excess binders, iron oxide and other oxides such as manganese, the sands should be thermally reclaimed.

Additionally, the sand size distribution could be altered so that there would be a higher packing efficiency, which would retard the ability of the sand to sinter and densify. However, this would lead to less permeability and in turn more gas defects in the casting. The other option is a mono-sized particle distribution. If a molding sand with a similar size was used, permeability would be very high while the packing efficiency would be very low. Because of the poor packing efficiency, there would be a smaller number of contact points and the effects of sintering would be reduced.

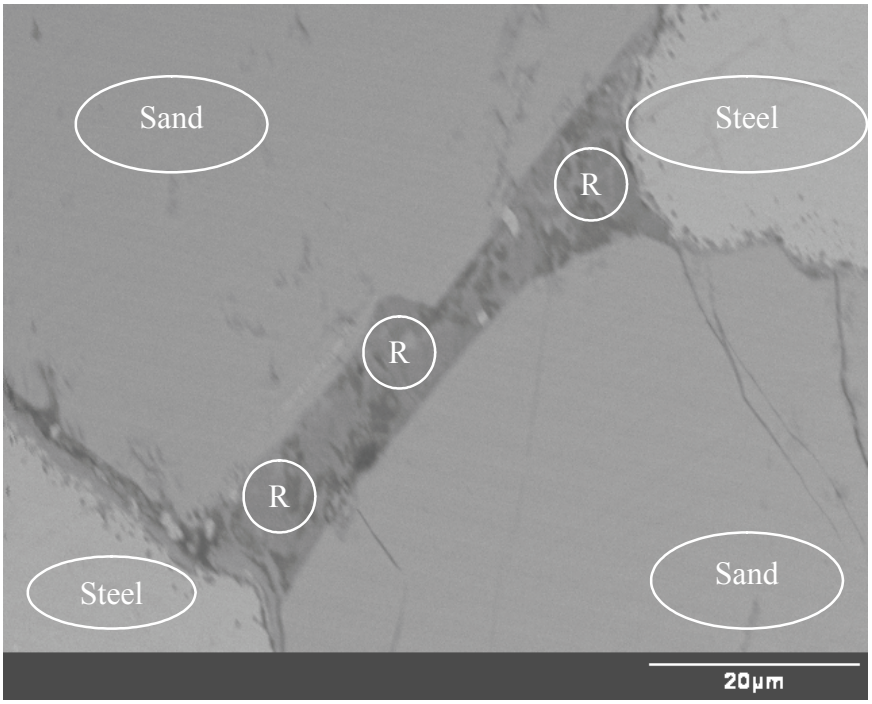

Figure 9: Backscattered electron (BSE) image of the burn-in sample from Foundry E. The sand grains appear joined to each other by a reaction product 'R'

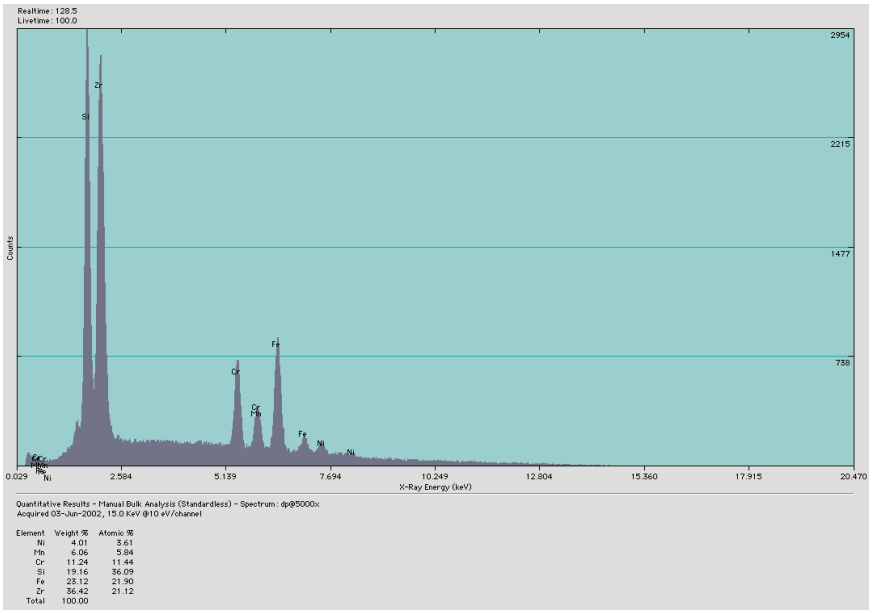

Figure 10: Energy dispersive spectrometer (EDS) analysis of the reaction product in the region of join of sand grains from the burn-in sample from Foundry D

Table 7: Approximate Composition of the Reaction Product Formed at the Region of Join of Sand Grains

Element	Weight %	Atomic %	Oxide %
Fe	23.12	21.9	20.15
Mn	6.06	5.84	5.3
Cr	11.24	11.44	9.95
Si	19.16	36.09	27.78
Zr	36.42	21.12	33.34
Ni	4.01	3.61	3.45

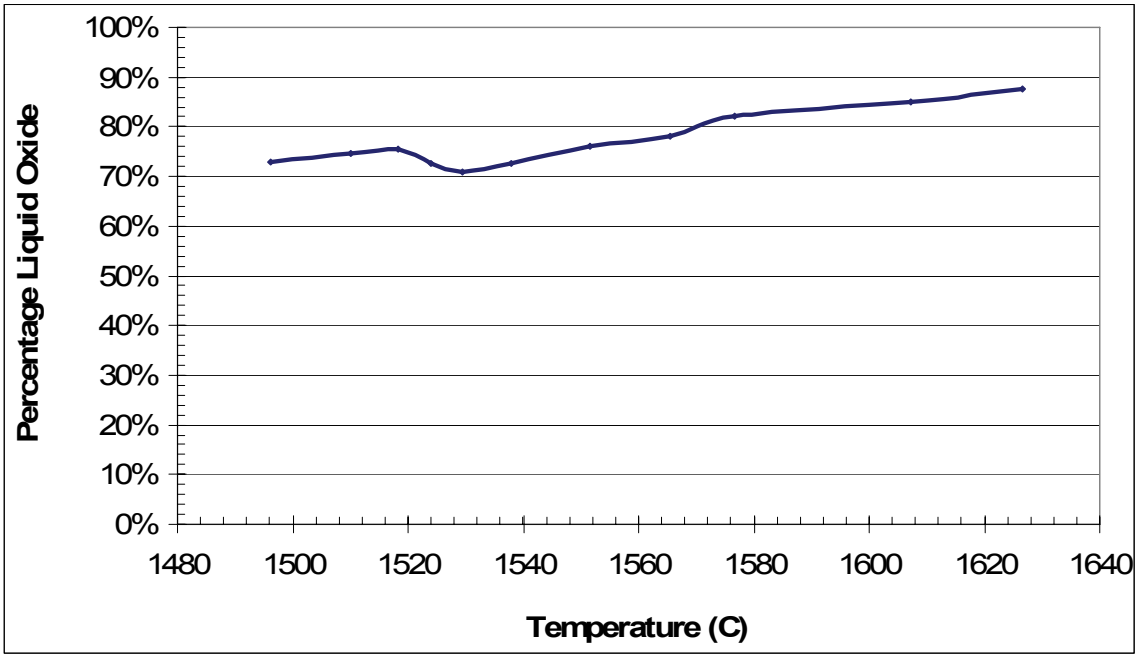

Figure 11: Thermodynamic analysis of the reaction product in Figure 10 shows that it was around 80 % liquid at steel pouring temperatures

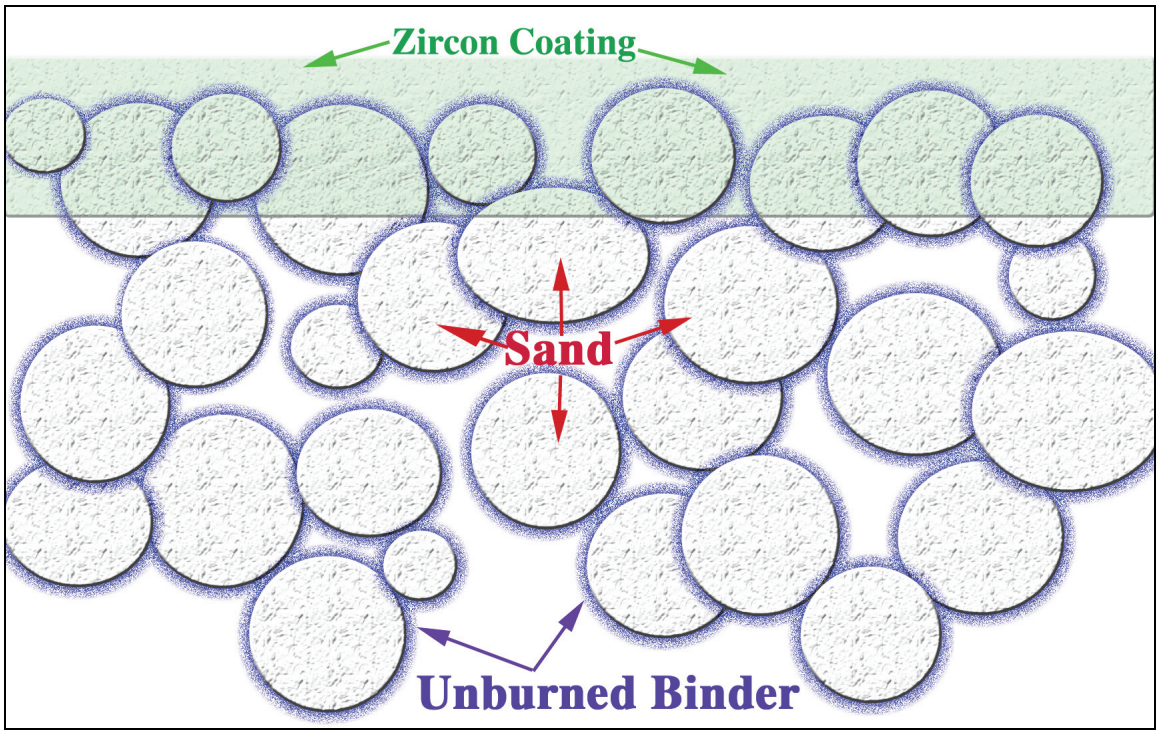

Figure 12: Sketch of zircon wash and silica sand interface

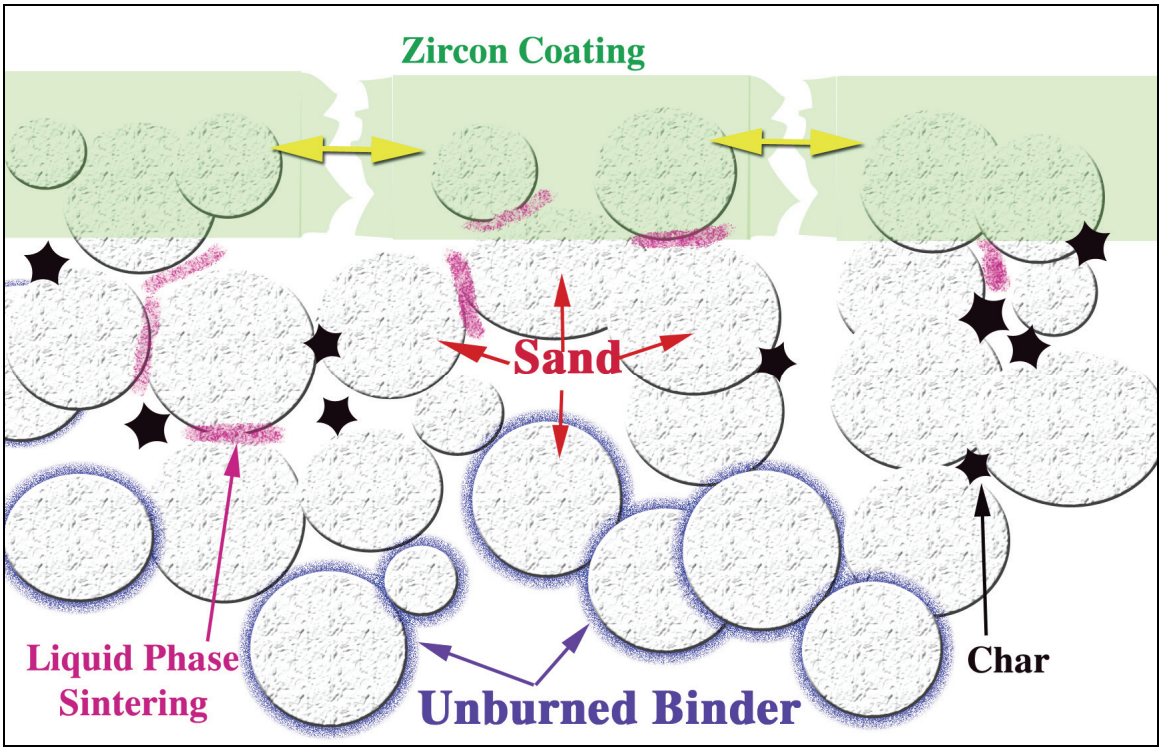

Figure 13: Sketch of liquid phase sintering in sand leading to cracks in zircon wash. Note the undecomposed binder remains at some distance for the mold surface but decomposes thermally near the mold cavity when metal enters

The existence of excess amounts of iron oxide, and manganese oxide facilitate liquid phase sintering. This would cause a significant amount of sand rearrangement, and non-uniform localized strain. The local strain would be enhanced by the additional volume change due to the decomposition of the carried-over binder residue. These two effects would create local tensile stresses and ultimately breaches in the zircon coating.

The importance of maintaining the integrity of the zircon wash stems from the inability of the metal to penetrate the sand pore structure. The pressure required to penetrate the mold can be estimated by referring to Equation 1. If the pressure (*P)* and the surface tension (γ) are held constant, the radius of the pore is the limiting factor on whether metal will penetrate into the mold. Zircon washes are so effective in preventing burn-in/on and penetration because of not only their resistance to chemical-reaction penetration, but also liquid state penetration. Zircon washes have a pore size that is about two orders of magnitude smaller than most production silica sands. This allows them to resist liquid state penetration as long as they are not breached.

$$\Delta P = \frac{2\gamma}{r} \qquad \text{Equation 1}$$

In fact, the pressure required to penetrate pores in typical zircon wash microstructures has been estimated to be equivalent to the static pressure from a 33-foot column of liquid steel (Richards, 1999). However, the pressure head to penetrate typical mold and core porosity was also estimated to be about equivalent to a two-inch column of liquid steel, based primarily on the pore size. Looking again at Equation 1, the sulfur has the effect of lowering the metal surface tension, γ, further acting to promote the penetration once the coating breaks.

Microstructural analysis of a large number of case studies suggested that the range of mold metal interaction defects from core penetration through burn-on to burn-in are all related to disruption of refractory mold washes in modern steel foundry no-bake practice (Richards, 2002). The finishing department definition of these defects often relates to the area density of metal connection through the coating rather than the existence of a reactive oxide liquid at the surface.

CONCLUSION

Burn-in, burn-on and metal penetration in coated no-bake molds appear to be part of the same range of events with the difference in severity related to area density of coating disruptions. The predominant mechanisms for burn-on and burn-in are most likely to be mechanical penetration through the zircon washes caused from the instability of the underlying silica sand. The instability and rearrangement of silica sand was an effect of liquid phase sintering sand due to excess accumulated iron and manganese oxide and volume changes due to decomposition of binder carry-over. These oxide impurities and binder carry-over can be eliminated by mechanically reclaiming followed by thermally reclaiming all spent foundry sands. If these impurities are eliminated, a stable foundation for zircon washes will be established, reducing the chances for mechanical penetration, burn-on and burn-in.

ACKNOWLEDGMENTS

The authors wish to acknowledge the financial support for this project from the AMC program through Steel Founders' Society of America. The technical interaction with the engineers and operating personnel at the participating foundries was very important in this program. We also appreciate the in-kind support in materials and production time at those foundries to test our findings and develop a "real world" basis for the result.

REFERENCES

Asanti, P., "Burn-on in Steel Castings," *Modern Castings*, Vol.49, pp 71-73, Issue 4 (1966)

Chernogorov, Vassin and Nikifor, A.P., "Investigation of Physical-Chemical Processes of Burn-on Formation on Steel Castings," *Cast Metals Research Journal*, Vol.6, pp 58-62, No.2 (1970)

Richards, V.L. and Rasquinha, D., "Burn-in/Burn-on: Case Study Findings," Proceedings *of the Steel Founders' Society of America Technical and Operating Conference*, Paper 4.6 (2002)

Richards, V. L. and Monroe, R. W., "Control of Metal Penetration in Steel Castings Production," Proceedings *of the Steel Founders' Society of America Technical and Operating Conference*, Paper 5.1 (1999)

Rowley, M. T., ed., *International Atlas of Casting Defects*, pp 200-205, American Foundrymen's Society, Inc., Des Plaines, IL (1993)

Svoboda, J.M., "Mechanisms of Metal Penetration in Foundry Molds," AFS *Transactions*, vol 102, pp 461-471, Paper 94-24 (1996)